Theory of Force Regulation by Nascent Adhesion Sites

Robijn Bruinsma
Department of Physics and Astronomy, University of California at Los Angeles

ABSTRACT The mechanical coupling of a cell with the extracellular matrix relies on adhesion sites, clusters of membrane-associated proteins that communicate forces generated along the F-Actin filaments of the cytoskeleton to connecting tissue. Nascent adhesion sites have been shown to regulate these forces in response to tissue rigidity. Force-regulation by substrate rigidity of adhesion sites with fixed area is not possible for stationary adhesion sites, according to elasticity theory. A simple model is presented to describe force regulation by dynamical adhesion sites.

INTRODUCTION

Adhesion sites and force regulation

The production of mechanical force by motor proteins has become a textbook staple of biological physics but the regulation of these forces has received much less attention in the physics literature. An important example of cellular force-regulation is encountered in *adhesion sites* (1). Adhesion sites are micron-size protein clusters linking the cytoskeleton to the extracellular matrix (ECM) that fills the space between cells. Forces generated inside cells along F-Actin filaments by Myosin II motor proteins are transmitted to the ECM via these adhesion sites (2). Adhesion sites pass through different stages of development. Initial adhesions or IAs (3) form at the outer edge of the lamellipodium of a cell. They are relatively simple structures consisting of integrin transmembrane proteins linked outside the cell to specific ECM ligands (such as fibronectin) and inside the cell to the adaptor protein Talin I that also binds actin filaments (see Fig. 1 and Refs. 4,5). The link between an IA and the actin filaments is weak and can slip under an applied force in the picoNewton (pN) range (6), an effect sometimes referred to as ''a slipping clutch''. IAs can mature to *focal complexes* (FCs), located somewhat further from the edge (we will refer to IAs and FCs together as ''nascent'' adhesion sites). FCs are bound to the cytoskeleton by a reinforced link—the clutch has ''engaged'' —and contain a larger number of constituent components, such as Vinculin (see Fig. 1), and apply an appreciable force, in the nanoNewton (nN) range (7), to the substrate. FCs provide purchasing points for traction forces exerted by migrating cells on the substrate (8). Finally, fully mature adhesion sites (*focal adhesions* or FAs) are large, complex structures that are important centers of cell signaling.

The regulation of adhesion site development is largely determined by *mechanical force*. Normally, this is the traction force applied by Myosin II motor proteins on the actin filament system connected to the site, but external forces also can stimulate development (9). It is well known that the size of mature FAs reversibly increases and decreases as a function of applied force (1). The force regulation of nascent adhesion sites (IAs and FCs) takes a different form: nascent adhesion sites match the force they exert to the stiffness of the substrate (10,11). Increased substrate stiffness stimulates development of IAs to FCs and causes a large increase in the force level applied by the cell to the substrate, from picoNewtons to nanoNewtons. This dependence of the force level on substrate rigidity is, for instance, responsible for *durotaxis* (12): a cell navigating over a heterogeneous substrate is guided by substrate elastic rigidity. It also provides a mechanism for the guidance of cell development by mechanical interactions with the surrounding tissue. Unlike the force regulation mechanism of mature FAs, the reinforcement of nascent adhesion sites does not depend on changes in size of the adhesion site. Optical trap assays using micron-sized, ligand-covered beads of fixed surface area exhibit the same reinforcement phenomena as actual adhesion sites (10).

Adhesion site development and elastic stress

The activation and reinforcement of IAs has been found to depend on chemomechanical activity localized to the adhesion site (10). The specific pathway is not fully known, but it is believed to involve phosphatase activity triggered by a force-induced conformational change of the integrin proteins (13,14). From a physical viewpoint it is quite surprising that substrate rigidity can regulate the reinforcement of an adhesion site. Adhesion sites are either stationary with respect to the substrate or motile (15). Newton's action-reaction principle seems to demand that the reaction force exerted by the ECM on a stationary adhesion site has to be equal and opposite to the traction force, the total external force applied by actin/Myosin contractile activity on the adhesion site. This latter force is generated inside the cell, far from the adhesion site, and a priori, should not depend on the elastic rigidity of the ECM. Substrate deformations generated by stationary adhesion sites have been measured using

Submitted June 24, 2004, and accepted for publication April 5, 2005.

Address reprint requests to Robijn Bruinsma, Tel.: 310-825-8539; E-mail: bruinsma@physics.ucla.edu.

0006-3495/05/07/87/08 $2.00

doi: 10.1529/biophysj.104.048280

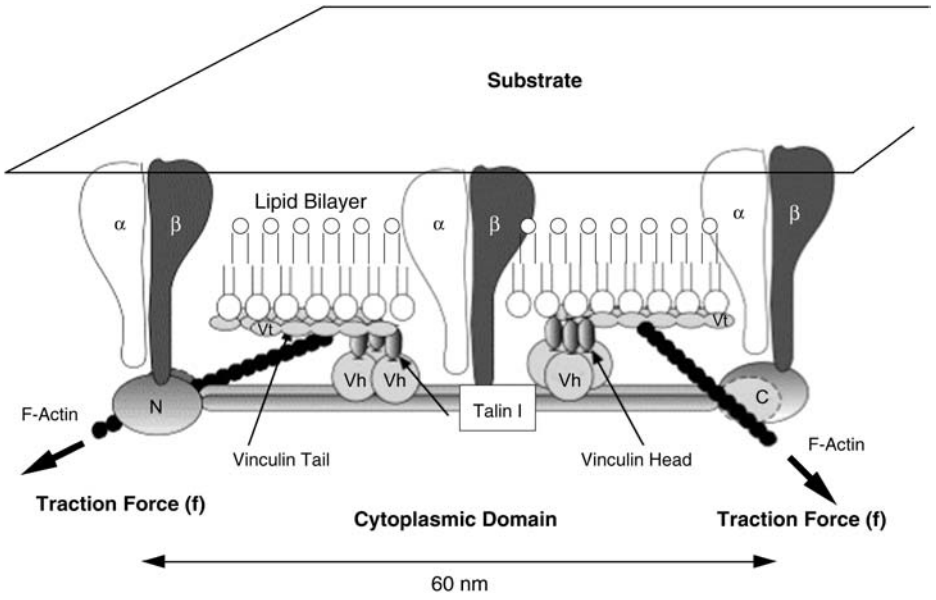

FIGURE 1 Initial adhesion site. Dimeric integrin transmembrane proteins bind to specific substrate ligands, such as fibronectin, as well as to the Talin I adaptor proteins of the cytoplasm. Talin I, in turn, is linked to the actin filaments of the cytoskeleton along which traction forces are generated. Reinforcement of the adhesion site involves recruitment of Vinculin proteins (figure adapted from Ref. 4).

patterned, deformable gels. The results are consistent with the predictions of continuum elasticity theory for the strain of a point source subject to an applied force (16). Now, as discussed in Appendix A, it follows from continuum elasticity theory that the stress distribution of an elastic medium subject to a localized external force exerted on the surface does not depend on the rigidity of the medium. This means that the reaction forces exerted by the substrate on a stationary adhesion site (and its proteins) do not depend on the substrate rigidity, so the activation of a stationary adhesion site containing force-sensitive proteins cannot be regulated by substrate rigidity.

The aim of the article is to propose a tractable physical model that describes the transition from IAs to FCs for dynamic adhesion sites (of fixed area). The model and its assumptions are described in A Two-State Model for Nascent Adhesion Sites. The analytical treatment is given in Methods, below, for readers with a background in statistical mechanics. Results and Discussion describes the results of the Methods section and addresses the question of how dynamical adhesion sites can be activated by substrate rigidity, followed by predictions that can be tested by micromechanical methods.

A TWO-STATE MODEL FOR NASCENT ADHESION SITES

Description of the model

The model assumes that the adhesion site can be in only one of two collective states: passive and active. The passive state corresponds to an IA connected via a weak slip link to an actin filament bundle parallel to the surface. The filament bundle is subject to a constant, external traction force T. The active state corresponds to an FC connected via a reinforced link to the filament bundle. The link between adhesion site and filament bundle is described by a two-state potential energy of mean force that depends on the status of adhesion site. Site activation is treated as a rapid, reversible chemical reaction between two states. The activation reaction is assumed to involve a conformational change of the adhesion site integrins (17), such that the reaction free energy includes the mechanical work performed by the applied force during the conformational change.

The adhesion site is assumed to be subject to three forces: 1), a force by the link potential that connects the adhesion site to the filament bundle; 2), a viscoelastic force exerted by the ECM on the site; and 3), a random thermal force. ECMs have complex rheological properties, as do actin networks. We will assume a very simple case, namely a substrate that can be treated as a Voigt-Kelvin body. For the present case, this means that the substrate exerts an elastic restoring force on the adhesion site as well as a Newtonian viscous drag. The mechanical properties of the filament bundle also are described in the simplest possible terms. The bundle is assumed to be subject to four forces: 1), the constant traction force; 2), a Newtonian viscous drag by the cytoplasm; 3), the link force of the adhesion site; and 4), a random thermal force. Finally, an important assumption of the model is that the equilibration time for activation, which has been measured to be of the order of 1–10 s (10), is due to mechanical relaxation and not chemical equilibration.

Under these assumptions, it is possible to obtain an expression for the typical force level exerted on the substrate by the adhesion site using the methods of statistical mechanics as discussed in Methods, below. In Appendix B we discuss the validity of the assumptions and typical parameter values of the model.

Methods

Denote the two adhesion site states as $S = -1$ (passive) and $S = 1$ (active). Let ΔG be the Gibbs free energy difference between the two states in the absence of applied force. ΔG is proportional to the number of integrins of the site and, in general, can depend on the concentration of reactants involved in the activation reaction. Let F be the force applied to the adhesion site by the link between the adhesion site and the cytoskeleton. We shall see that, in general, F need not equal the traction force T for a dynamic adhesion site. The thermodynamic work by the external force during the conformational change of the integrins is then $F\ d^*$, which is where d^* is a length scale characterizing the molecular displacement of the integrins during the conformational change. Under conditions of chemical equilibrium, the expectation value of the site variable is given by

$$\langle S\rangle_F = \tanh\frac{1}{k_B T}[-\Delta G + F d^*]. \tag{1}$$

The activation/deactivation reaction is here assumed to be cooperative (see Appendix B), as is for instance believed to be the case for clusters of chemoreceptor proteins (18). In the opposite case, e.g., if the activation reactions of the different integrin/phosphatase complexes of an adhesion site are not correlated, then the argument of Eq. 1 should be divided by the number of integrins of the site.

The adhesion site can move along the filament bundle direction (x direction), and the position of the site is denoted by $X(t)$. The filament position along the x direction is denoted by $Z(t)$, with $X(t = 0) = Z(t = 0) = 0$. The filament bundle is also exposed to a traction force T along the x direction. The link between bundle and site is described by a potential of mean force $U(\rho,S)$ with $\rho(t)$ the relative displacement $Z(t)$–$X(t)$ between bundle and site. The potential energy also depends on the site variable S and has the following general properties: 1), the absolute minimum of $U(\rho,S)$ with respect to ρ is located at $\rho = 0$, and 2), $U(\rho,S) \to 0$ for large $|\rho|$. The range of the potential is denoted by ρ_f. The activation energy for escape out of the potential well is denoted by ΔU for $S = -1$ and by $\Delta\Delta U$ for $S = 1$. We will assume that $\Delta U/\rho_f \ll T$, which means that in the passive $S = -1$ state, the force of the link potential is weak compared to the traction force T. The activation barrier $\Delta\Delta U$ of the active $S = 1$ is assumed large compared to ΔU.

Turning to the equation of motion of the adhesion site, the substrate—a Voigt-Kelvin body by assumption—exerts a harmonic restoring force $-kX$ and a viscous drag $\gamma_B(dX/\,dt)$ on the adhesion site. The spring constant equals $k \approx Ya$, with Y the Young's Modulus of the substrate—the rigidity that is supposed to be measured by the nascent adhesion site—and with a as the adhesion site diameter. The friction coefficient equals $\gamma_B \approx \eta a$, with η the substrate viscosity. The equation of motion of the site is then

$$\gamma_B\frac{dX}{dt} + kX = \frac{dU(\rho,S)}{d\rho} + f(t). \tag{2}$$

Here, $f(t)$ describes the thermal random noise force exerted on the site. According to the fluctuation-dissipation theorem, the noise autocorrelation function obeys the condition

$$\langle f(t)f(0)\rangle = 2\gamma_B k_B T\,\delta(t). \tag{3}$$

The equation of motion of the bundle is obtained in a similar way by setting the sum of the forces on the bundle equal to the viscous drag on the bundle,

$$\gamma_R\frac{dZ}{dt} = -\frac{dU(\rho,S)}{d\rho} + T + f^*(t). \tag{4}$$

Here, $f^*(t)$ is the thermal fluctuation force on the bundle, which obeys a condition similar to Eq. 3. Note that if $U'(\rho,S) = 0$ (i.e., no link) then the filaments are dragged along with a velocity V_R. We identify V_R with the (measured) retrograde flow velocity of actin filaments inside the lamellipodium, so $\gamma_R = T/V_R$.

After addition of Eqs. 2 and 4 and integration, one can express the site displacement $X(t)$ in terms of the relative displacement $\rho(t)$,

$$X(t) = \frac{1}{\gamma_R + \gamma_B}\int_0^t dt'\,\exp^{-(t-t')\left[\frac{k}{\gamma_R+\gamma_B}\right]} \times\left\{T - \gamma_R\frac{d\rho(t')}{dt} + f(t') + f^*(t')\right\}. \tag{5}$$

Note that Eq. 5 does not depend on the link potential. If $t \ll \tau$, with $\tau = (\gamma_R + \gamma_B)/k$ the mechanical relaxation time, then Eq. 5 reduces to

$$X(t) \approx \frac{V_R\,t}{1+\gamma_B/\gamma_R} - \frac{\rho(t)}{1+\gamma_B/\gamma_R} + \frac{1}{\gamma_B+\gamma_R}\int_0^t dt'(f(t') + f^*(t')), \tag{6}$$

using $\gamma_R V_R = T$. The next steps simplify for $\gamma_B \ll \gamma_R$ (the opposite case does not present new features). Inserting Eq. 6 in Eq. 5, and using $\gamma_B \ll \gamma_R$, we obtain the following equation of motion for the relative displacement $\rho(t)$ if $t \ll \tau$,

$$\gamma_B\frac{d\rho}{dt} + k(\rho - V_R\,t) \cong -U'(\rho,S) + \gamma_B V_R + f(t). \tag{7}$$

Equation 7 is the Langevin equation of motion of a particle with coordinate $\rho(t)$ moving in a potential well $U(\rho,S)$ subject to a constant force $\gamma_B V_R$, a harmonic restoring force and a time-dependent force $F_{ex}(t) = kV_R t$. The effective potential energy $U(\rho,S) + (1/2)k(\rho - V_R t)^2$ has the form of a double-well potential with one minimum (ρ_1) near $\rho = 0$ and a second minimum (ρ_2) near $\rho = V_R t$. The first minimum corresponds to an adhesion site bound to the filament and the

second minimum to a dissociated site. As $F_{ex}(t)$ grows with time, the second minimum becomes more dominant and, eventually, a transition from the first to the second minimum must take place. For the $S = -1$ passive case, the characteristic timescale for the transition between these two states must be less than τ. The reason is that the applied force $F_{ex}(t = \gamma_R/k) = V_R\gamma_R$ at time $t = \tau$ for a site in the first minimum $\rho = \rho_1$ equals the traction force T. By assumption, the traction force T significantly exceeds the maximum restoring force, of order $\Delta U/\rho_f$, that the potential well can exert in the passive state. This means that the adhesion site must have dissociated before $t = \tau$. If, on the other hand, the maximum restoring force $\Delta\Delta U/\rho_f$ of the active case, with $S = 1$, significantly exceeds T, then an $S = 1$ site is not expected to dissociate before $t = \tau$. The filament bundle is arrested in this case and the full traction force T is exerted on the adhesion site.

We are interested in the most likely force $\langle F(k)\rangle$ exerted on the adhesion site at the moment of dissociation. If we assume that, following dissociation, the adhesion site will rebind to actin filaments, then this $\langle F(k)\rangle$ can be considered as the typical maximum force that is exerted on the adhesion site during a dissociation/rebinding cycle. Applying Kramer's method for computing escape probabilities out of a potential well (19) to Eq. 7, we find for $\langle F(k)\rangle$,

$$\langle F(k)\rangle \approx f_\beta \ln\left\{\frac{kV_R}{J_0 f_\beta}\right\} + \frac{\langle \Delta U\rangle}{\rho_f}. \quad (8)$$

Here, $f_\beta = k_BT/\rho_f$ is the thermal force for bond dissociation, whereas J_0 is the attempt rate for escape out of the well. This attempt rate depends on the second derivatives of $U(\rho)$ at $\rho = 0$ and at $\rho = \rho_f$, on the friction coefficient γ_B, and on temperature, but we will not require an explicit expression. Finally, $\langle \Delta U\rangle$ is the expectation value of the activation energy of the potential during dissociation. If the relaxation time of the coordinate $\rho(t)$ is sufficiently long compared to the chemical equilibration time of the site variable S, then $\langle \Delta U\rangle$ is the thermal average of the passive and active activation energies for $S = -1$, respectively, $S = 1$,

$$\langle \Delta U\rangle = \Delta U + 1/2\ \Delta\Delta U(1 + \langle S\rangle_F), \quad (9)$$

with F, as before, the force applied to the adhesion site by the link potential. If we equate the F in Eq. 9 with the dissociation force $\langle F(k)\rangle$ of Eq. 8, then Eqs. 1, 8, and 9 constitute a set of coupled equations. They can be combined into a single self-consistency condition for $\langle F(k)\rangle$, which is simplified by introducing dimensionless quantities. Using a force scale $f_\beta = k_BT/\rho_f$, a stiffness scale $k_0 = (J_0 f_\beta/\ V_R)\ \exp^{-\beta\Delta U}$, and an energy scale k_BT, the self-consistency condition reads

$$\tilde{F}(\tilde{k}) \approx \ln\tilde{k} + \frac{\Delta\Delta\tilde{U}}{2}\{1 + \tanh[(\tilde{F}(\tilde{k}) - \tilde{F}_c)d^*/\rho_f]\}. \quad (10)$$

Here, $F_c = \Delta G/d^*$ is the force level such that the free energies of the active and passive states are degenerate. Dimensionless quantities are marked with an accent.

RESULTS AND DISCUSSION

The analysis of the two-state model, given in Methods, leads to the following scenario. Assume that at time $t = 0$ a weak slip-link between an adhesion site and a filament bundle is formed (an IA). With time, the retrograde motion of the filaments drags the adhesion site along the direction of the moving filament through the link potential. In response to the motion, the elastic reaction force exerted on the site by the substrate starts to rise. What will happen next is dependent on the rate at which this force is rising with time, the *force loading-rate*. The force loading-rate, in our case, is proportional to the Young's Modulus Y of the substrate, the size a of the adhesion site, and the retrograde velocity V_R of the actin filaments. For soft substrates, the force loading-rate is low and the site will dissociate from the filaments at a low reaction force level (see Eq. 8). After dissociation, the adhesion site can rebind ''downstream'' to the filament and the cycle can restart. For more rigid substrates, on the other hand, the force loading-rate is higher and the associated dissociation force level is higher as well (see Eq. 8). If the dissociation force level exceeds the force level required for the site activation reaction, then the link is reinforced and the filament bundle ''locks'' to the adhesion site. The retrograde motion of the filament is arrested and the full traction force T is applied to the adhesion site.

These two scenarios are illustrated graphically in Fig. 2, which shows the solution of the self-consistency condition, Eq. 10. The stiffness parameter k of the horizontal axis is proportional to the rigidity of the substrate (i.e., the Young's Modulus). The vertical axis is the most likely force at the moment of dissociation of the adhesion site from the filament bundle. The force level of the lower branch of Fig. 2, which corresponds to an IA, exhibits a logarithmic dependence on the Young's Modulus for highly deformable substrates (small k-values). This logarithmic dependence has the same physical origin as the logarithmic dependence on force loading-rate of the well-known Bell-Evans expression for molecular dissociation forces (20). As the substrate rigidity increases, the dissociation force increases and for increasing k-value a threshold k_c is reached where the dissociation force level diverges. The threshold rigidity is $Y_c \propto \exp\{F_c/f_\beta\}$. Note that the threshold rigidity depends exponentially on the force level at which the energies of the active and passive states are degenerate. The upper branch of Fig. 2 corresponds to an activated adhesion site with a dissociation force that is not dependent on substrate rigidity. If the traction force T is less than the maximum restoring force of the reinforced potential, then this branch corresponds to a stationary site linked to an arrested filament bundle.

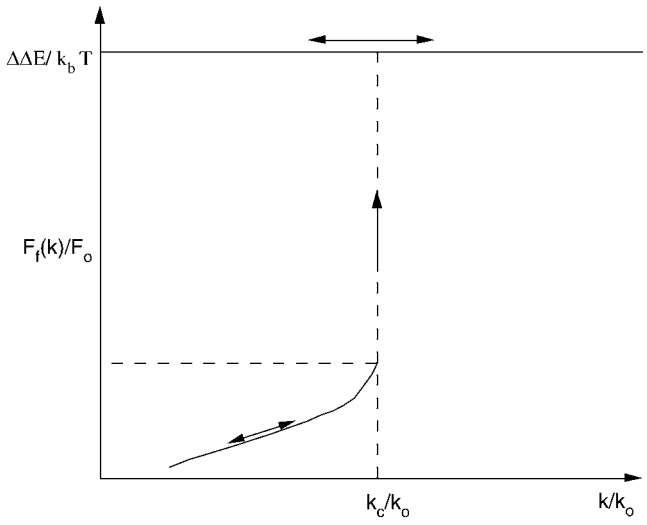

FIGURE 2 Dependence of the adhesion-site dissociation force on substrate stiffness obtained from Eq. 10. Vertical axis is the most likely dissociation force divided by the thermal force scale $f_\beta = k_B T/\rho_f$, with ρ_f the characteristic scale of the potential linking the adhesion site to the actin filament bundle. Horizontal axis is the substrate stiffness $k \approx Ya$, with Y the Young's Modulus, and a the adhesion-site dimension divided by the stiffness scale $k_0 = (Jf_\beta/V_R)$, with J the zero-force escape rate of the adhesion site in the slip state and with V_R the retrograde velocity. The lower branch corresponds to a slipping adhesion site, terminating at a critical stiffness. The upper branch corresponds to a reinforced state that fully transmits traction to the substrate. Once the system is reinforced, it will not return to the slip state.

How is it possible that the dissociation force of the lower branch depends on the substrate rigidity despite the action-reaction principle? This is a result of the fact that a slipping adhesion site is subject not only to the elastic reaction force of the substrate but also to viscous drag. Only the sum of the elastic reaction force and the viscous drag must equal the external traction force. There is no reason why the partition ratio between elastic and viscous forces could not depend on substrate rigidity, and indeed, it does for the model. Once the adhesion site is activated, reinforced, and immobilized, the dependence on substrate rigidity disappears, however.

The qualitative features of the simple two-state model appear to be surprisingly similar to the experimental observations as summarized in the Introduction: rigidity-dependent force regulation by adhesion sites is not in violation of fundamental physical principles. It should be clear, however, that the assumptions underlying the two-state model, as described in A Two-State Model for Nascent Adhesion Sites, do not do justice to the rich phenomenology of actual adhesion sites. For instance, the assumption of there being just two adhesion-site states is too simplistic to describe the complexity of the Src kinase/phosphatase and Rho-GTPase signaling pathways that are known to be involved in actual adhesion site activation (1), nor does the model account for the complex rheological properties of the ECM or the cytoplasm.

It is proposed, however, that certain general features are not expected to be sensitively dependent on these assumptions, and it is these features that should be verified experimentally. The claim that stationary adhesion sites of fixed area should not be involved in cellular force-regulation determined by substrate rigidity is such a general result —relying essentially only on the action-reaction principle —and it could be directly verified. The forces exerted by stationary adhesion sites have been measured by the bed-of-nails method (21) and—for larger adhesion sites—were found to be proportional to the adhesion site area. The measured slope is proportional to the force per integrin (see Appendix B). The prediction is that this slope should not be sensitive to the bending stiffness of the vertical columns, provided the sites are stationary. Note, though, that stationary adhesion sites very well could respond to changes in externally applied forces since that would increase the forces on the adhesion site proteins.

Next, the predicted logarithmic dependence of the slip force on substrate rigidity of slipping IAs is expected to be a robust feature that could be verified by optical trap assays of ligand-covered beads (see below). The most interesting general prediction of the model concerns, however, the reversibility of IA activation. Even though the chemical reaction describing transitions between active and passive states was assumed to be reversible, and in fact to be close to chemical equilibrium, the model predicts that the mechanical system as a whole is not reversible. Once an IA has been promoted to an FA under an increase in substrate rigidity, the adhesion site should, according to the model, remain reinforced after the rigidity is reduced. This is in contrast to the size regulation of mature FAs under external forces, which is reversible.

Physically, this irreversibility is a consequence of the fact that once the clutch has engaged, i.e., with the adhesion site locked to the filament bundle, the stationary site is now fully subject to the external traction T. For a stationary site, the reaction force must remain equal to T, even during a quasistatic reduction of the rigidity. This prediction could be directly tested in an optical bead assay. The stiffness constant of an optical trap—controlled by laser intensity—corresponds to the stiffness constant of the harmonic force and thus to the horizontal axis of Fig. 2. Assume that a ligand-covered optical bead is placed on the lamellipodium of a cell and captured by a stiff optical trap. After a waiting period of the order of the mechanical relaxation time, the force on the bead should start to rise as the adhesion molecules are getting activated and a link is established with the cytoskeleton. At this point the bead is released from the trap and carried along by the retrograde motion of the actin filaments. The two-state model now predicts that if this bead is captured once again by the trap, then the adhesion site still should be in the activated state and able to immediately apply the same external traction force to the bead. This prediction is at least qualitatively consistent with the observations reported in Ref. 10.

APPENDIX A: ELASTIC STRESS DISTRIBUTION OF STATIONARY ADHESION SITES

Assume that a bundle of actin filaments is attached to a stationary adhesion site. The substrate is assumed to be a semi-infinite, isotropic, homogenous elastic medium with a Young's Modulus Y and a (positive) Poisson Ratio σ_p. The substrate rigidity is determined by the Young's Modulus. The boundary conditions of the surface—the x,y plane—are that no external force is applied to the surface apart from a single site located at the origin. Away from the origin, the components $\sigma_{zi} = \sigma_{iz}$ of the stress tensor σ_{ij} are thus 0 at the surface ($n_j\sigma_{ij}$ is the force per unit area, along the i direction, applied to an area element with normal n_j). The traction force on the site is assumed to be directed along the x axis and is characterized by a local stress distribution $\sigma_{zx} = \sigma_0\,(x,y)$ whose area integral equals the traction force T.

The resulting elastic displacement of the substrate in the $z > 0$ half-space can be obtained by solving the classical equations of continuum elasticity theory. Specifically, the displacement u_x of the surface of the substrate along the x direction (i.e., the traction direction) at a distance $\vec{r}$ from the adhesion site can be shown to be (22)

$$u_x(\vec{r}) = \frac{(1+\sigma_p)}{\pi Y}\int d^2\rho\,\frac{\sigma_0(\vec{\rho})}{|\vec{r}-\vec{\rho}|}\left\{(1-\sigma_p) + \sigma_p\frac{(x-\rho_x)^2}{|\vec{r}-\vec{\rho}|^2}\right\}. \tag{A1}$$

The surface integral extends here over the area surrounding the origin where the force is applied. The key point is that u_x is inversely proportional to Y, which is true also for the y and z components of the displacement profile. According to Eq. A1, the displacement u_0 of the center of the adhesion site along the traction direction is of the order of

$$u_0 \approx \left(\frac{1}{Ya}\right)T \approx \left(\frac{\sigma_0}{Y}\right)a\ , \tag{A2}$$

with $a = A^{1/2}$ the characteristic dimension of the adhesion site (A is the area) and with σ_0 the spatial average of the externally applied stress over the area of the adhesion site, i.e., $\sigma_0 = T/A$. The substrate elastic reaction force on the site acts as a harmonic spring with a spring constant $k \approx Ya$ proportional to the Young's Modulus. Note that the adhesion-site displacement measured in units of a is of the order of the dimensionless ratio σ_0/Y of the applied stress and the Young's Modulus. One can obtain the value of the traction force T from a measurement of the elastic displacement field of the substrate, which is in fact a feasible procedure (16).

Geometrical deformations of the elastic medium are characterized by the strain tensor $u_{ij} = (1/2)\left(\partial_i u_j + \partial_j u_j\right)$, which can be obtained from the displacement field. The components of the strain tensor clearly are again inversely proportional to Y. The forces exerted by the substrate on the adhesion site are, however, determined by the stress tensor σ_{ij}, which is related to the strain tensor by

$$\sigma_{ij} = \frac{Y}{1+\sigma_p}\left(u_{ij} + \frac{\sigma_p}{1-\sigma_p}u_{ll}\delta_{ij}\right). \tag{A3}$$

Because the components of the strain tensor are inversely proportional to Y, it follows that the substrate stress tensor is independent of the Young's Modulus of the substrate. For example, far from the adhesion site, the σ_{xx} component of the stress tensor drops with distance as

$$\sigma_{xx}(x, y=0, z=0) \approx -\sigma_0\left[\frac{\sigma_p+2}{2\pi}\right]\left(\frac{a}{x}\right)^2. \tag{A4}$$

Equation A4 can be understood in terms of dimensional analysis. The substrate stress at a given location could depend on the externally applied stress σ_0, the elastic modulus Y of the substrate, the spatial distance r from the adhesion site, and the size a of the site. In view of the linearity of the equations of elasticity, the substrate stress must be proportional to the external stress σ_0 multiplied by some dimensionless function of the ratio (a/r). Far from the adhesion site, the stress should be proportional to the adhesion site area, again in view of the linearity, so this should be a quadratic function. It is not possible to construct a separate dimensionless factor that depends on the Young's Modulus Y and not on σ_0, so the stress must be independent of Y. In a more complex model, one might describe an adhesion site as a thin elastic plaque with a separate elastic modulus Y^*. In that case, the substrate stress, in principle, could depend on a separate dimensionless ratio (Y/Y^*). However, by applying the condition of stress continuity to the plaque, it follows that this dependence is absent.

APPENDIX B: NUMERICAL VALUES

In this Appendix we assign approximate numerical values to the physical quantities appearing in the model and discuss the various approximations.

The traction force T transmitted by adhesion sites has been measured for a variety of deformable substrates. The traction force of larger adhesion sites scales with the area A of the site (21) as $T = \sigma_0$ A. The mean stress level σ_0 is of order 1–5 nN/μ^2, ~1% of the stress of the actin/Myosin bundles of animal muscles. Assuming that the traction force is proportional to the number N of actin filaments linked to the site, then $T = N f_M$ where f_M is the traction force per filament. This unit traction must be of the order of the tension per unit area σ_0 times the area per filament. The spacing a_0 between the filaments of an F-Actin bundle cross-linked by α-actinin—an important component of FAs—is ~30 nm, whereas 30 nm also happens to be the spacing for both integrin and actin binding sites along the elongated Talin I adapter protein (see Fig. 1). For a_0 equal to 30 nm and an area per filament of order a_0^2, the unit force f_M is of the order of a few picoNewtons. The total number N of filaments per site, and presumably also the number of integrins, is then of the order of 10^3–10^4 for an adhesion site area of the order of 10 μm^2.

Although the rheological properties of model gels vary considerably, certain collagen gels indeed can be described as a Voigt-Kelvin body (23) with an elastic modulus Y in the range of kPa and an effective viscosity η in the range of 10^6 Pa s. This is a fairly typical Y value for the model gels used in the adhesion assays, although the rheological properties of actual ECMs vary greatly and normally are non-Newtonian. The dimensionless site displacement $u/a = \sigma_0/Y$ of Appendix B, the typical substrate strain level near an adhesion site, would then be of the order of 1 and the spring constant k would be in the range of pN/nm for a 1-μm site. This is also the order of magnitude of the stiffness of optical traps. The friction coefficient $\gamma_B \approx \eta a$ for a 1-μm adhesion site would be of order 10^4 pN s/nm. For an optical trap in aqueous medium, the friction coefficient of the bead would be negligible compared to γ_R, which is estimated as follows. The actin retrograde flow velocity V_R is in the range of μm/min, so the force loading rate kV_R is in the range of 15 pN/s, and therefore the effective friction coefficient per filament $\gamma_R = f_M/V_R$ should be of the order of 0.1 pN s/nm. The mechanical relaxation time $\tau = \gamma_R/k$ would be of the order of 0.1-s times the number of filaments. The assumption $\gamma_R \gg \gamma_B$ we made for convenience holds for optical beads but may fail for gels.

A key assumption of the theory is that the chemical equilibration time should be less than the mechanical relaxation time, i.e., the rate-limiting step for activation must be mechanical relaxation and not chemical equilibration. From optical bead model studies (10), it is known that the rate-limiting step for IA to FC switching is of the order of 1–10 s. The predicted mechanical relaxation time $\tau = \gamma_R/k$ is of order 0.1-s times the number of filaments or complexes, using the earlier estimates. For 10^2–10^3 filaments per site, this mechanical relaxation time is of the order of 10–100 s, which is in reasonable agreement with the measured relaxation time. It is thus at least consistent to assume that the mechanical degrees of freedom indeed are slow compared to the chemical equilibration rates.

Values for the most likely dissociation force $\langle F\rangle$ of single molecular links can be obtained from single-molecule micromechanics. A recent single-molecule study of the interaction between individual $\alpha_4\beta_1$ integrins and VCAM ligands (E. Evans, unpublished) reports that the Bell-Evans relation holds for that case with a thermal force scale $f_\beta = k_B T/\delta_f$ of ~13 pN and

a zero-force dissociation rate J (i.e., off-rate) in the range of 0.1–1/s depending on condition. For a loading rate of 10 pN/s, the dissociation force is then in the 1–10 pN range. Assuming an attempt rate J_o for dissociating weak protein/protein links to be in the (usual) range of 10^9 Hz would mean that the single-link activation energy ΔU of an integrin/VCAM pair is in the range of 20 k_BT. For a reinforced integrin dimer, the dissociation force was indeed found to be much larger, in the range of 50–100 pN, and relatively independent of the force loading-rate (E. Evans, unpublished), consistent with the two-state model. This would correspond to a reinforced binding energy of the order of 100 k_BT. Single-molecule studies of the strength of the integrin/Talin link are currently not available. The generalization from single-molecule studies to clusters of links is complicated by the fact that this depends sensitively on whether the links act mechanically in parallel or in series (24). For N cooperative links acting in parallel, the thermal force level should be that of a single link, whereas the off-rate should be $J = NJ_0 \exp^{-N\Delta U/k_BT}$ in terms of the single-molecule quantities. Note that for large N this would greatly increase the dissociation force. For a noncooperative, zipper-type bond dissociation, the thermal force in Eq. 11 should be N times the single-molecule force level f_β, whereas $J \approx (J_0/N)\exp^{-\Delta U(\delta_f)/k_BT}$. In view of these, and other uncertainties, we refrain from making quantitative estimates of the critical force for unbinding and the critical Young's Modulus. It clearly would be extremely useful if the model studies of the slip state could be repeated for different stiffness constants of the trap to check whether the Bell-Evans relation holds for slipping IAs.

The zero-force free energy difference ΔG of an adhesion site between the active and passive states can be estimated by recalling that the characteristic force level f_p exerted on a reinforced complex is of the order of pN per filament. To estimate the mechanical work during activation, we need to know the conformational changes of actin-bound adhesion site integrins during activation, which currently are not known. Conformational changes of integrins upon ligand binding were examined in solution studies (17), who found that the β-integrin tail, which is linked to the Talin adapter in adhesion sites, can undergo a large rotation between competing ''open'' and ''closed'' conformers. The associated displacement of the tail end is unusually large, ~10 nm. If rotation of the β-integrin tail is indeed the conformational change that is linked to integrin activation, then the mechanical work $f_p\, d^*$ per site available for activation would be of the order of 10 k_BT. This must exceed the zero-force reaction free energy ΔG per integrin. It follows that the integrin/phosphatase complex must be a very sensitive mechanosensor as it apparently operates barely above the thermal noise level.

APPENDIX C: LIST OF SYMBOLS

a	Size of the adhesion site.
d^*	Molecular displacement of the integrin (β-subunit) during activation.
η	Substrate viscosity.
$f(t)$	Random thermal force.
f_β	Thermal force for bond dissociation.
F	Force applied by the link potential between the adhesion site and the actin filaments.
γ_B	Friction coefficient of the adhesion site.
γ_R	Friction coefficient of the actin filament.
ΔG	Gibbs free energy difference between activated and passive states of the adhesion site in the absence of an applied force.
J_0	Attempt rate for escape out of the link potential.
k	Spring constant of the adhesion site.
k_BT	Thermal energy.
ρ_f	Relative displacement of the adhesion site and the filament.
ρ	Range of the link potential energy.
σ_{ij}	Stress tensor.
σ_0	Traction force per unit area.
σ_p	Poisson's Ratio.
S	Adhesion site state variable.
T	External traction force applied on the actin filament by Myosin II activity.
τ	Mechanical relaxation time.
$U(\rho,S)$	Link potential.
ΔU	Activation energy of the link potential in the passive state.
$\Delta\Delta U$	Activation energy of the link potential in the active state.
V_R	Retrograde velocity.
$X(t)$	Position of the adhesion site.
$Y(t)$	Filament bundle position.
Y	Young's Modulus of the substrate.
$Z(t)$	Relative displacement between actin bundle and adhesion site.

I thank S. Bershadsky, T. Bickel, B. Geiger, M. Kozlov, A. Nicolas, S. Safran, U. Schwarz, and M. Sheetz for many useful discussions and E. Sackmann for a critical reading.

REFERENCES

1. Geiger, B., and A. Bershadsky. 2001. Assembly and mechanosensory function of focal contacts. *Curr. Opin. Cell Biol.* 13:584–592.
2. Oliver, T., M. Dembo, and K. Jacobson. 1995. Traction forces in locomoting cells. *Cell Motil. Cytoskeleton.* 31:225–240.
3. Izzard, C. 1998. A precursor of the focal contact in cultured fibroblasts. *Cell Motil. Cytoskeleton.* 10:137–142.
4. Critchley, D. 2000. Focal adhesions—the cytoskeletal connection. *Curr. Opin. Cell Biol.* 12:133–139.
5. Nayal, A., D. J. Webb, and A. F. Horwitz. 2004. Talin: an emerging focal point of adhesion dynamics. *Curr. Opin. Cell Biol.* 16:94–98.
6. Jiang, G., G. Giannone, D. Critchley, F. Fukumoto, and M. Sheetz. 2003. Two-picoNewton slip bond between fibronectin and the cytoskeleton depends on talin. *Nature.* 424:334–337.
7. Galbraith, C. G., K. M. Yamada, and M. P. Sheetz. 2002. The relationship between force and focal complex development. *J. Cell Biol.* 159:695–705.
8. Lauffenburger, D., and A. Horwitz. 1996. Cell migration: a physically integrated molecular process. *Cell.* 84:359–369.
9. Riveline, D., E. Zamir, N. Q. Balaban, U. S. Schwarz, T. Ishizaki, S. Narumiya, Z. Kam, B. Geiger, and A. D. Bershadsky. 2001. Focal contacts as mechanosensors: externally applied local mechanical force induces growth of focal contacts by an mDia1-dependent and ROCK-independent mechanism. *J. Cell Biol.* 153:1175–1186.
10. Choquet, D., D. Felsenfeld, and M. Sheetz. 1997. Extracellular matrix rigidity causes strengthening of integrin-cytoskeleton linkages. *Cell.* 88:39–48.
11. Pelham, R., and Y.-L. Yang. 1997. Cell Locomotion and focal adhesions are regulated by substrate flexibility. *Proc. Natl. Acad. Sci. USA.* 94:13661–13665.
12. Lo, C. M., H. B. Wang, M. Dembo, and Y. L. Wang. 2000. Cell movement is guided by the rigidity of the substrate. *Biophys. J.* 79: 144–152.
13. Schmidt, C. 1998. Mechanical stressing of integrin receptors induces enhanced tyrosine phosphorylation of cytoskeletally anchored proteins. *J. Biol. Chem.* 273:5081–5085.
14. Calderwood, D. 2004. Integrin activation. *J. Cell Sci.* 117:657–666.
15. Smilenov, L., A. Mikhailov, R. Pelham, E. Marcantonio, and G. Gundersen. 1999. Focal adhesion motility revealed in stationary fibroblasts. *Science.* 286:1172–1174.
16. Balaban, N. Q., U. S. Schwarz, D. Riveline, P. Goichberg, G. Tzur, I. Sabanay, D. Mahalu, S. Safran, A. Bershadsky, L. Addadi, and B. Geiger. 2001. Force and focal adhesion assembly: a close relationship studied using elastic micropatterned substrates. *Nat. Cell Biol.* 3:466–472.

17. Takagi, J., B. M. Petre, T. Walz, and T. A. Springer. 2002. Global conformational rearrangements in integrin extracellular domains in outside-in and inside-out signaling. *Cell*. 110:599–611.

18. Duke, T., and D. Bray. 1999. Heightened sensitivity of a lattice of membrane receptors. *Proc. Natl. Acad. Sci. USA*. 96:10104–10108.

19. Hänngi, P., P. Talkner, and M. Borkovec. 1990. Reaction rate theory: 50 years after Kramer's. *Rev. Mod. Phys*. 62:251–341.

20. Merkel, R., P. Nassoy, A. Leung, K. Ritchie, and E. Evans. 1999. Energy landscapes of receptor-ligand bonds explored with dynamic force spectroscopy. *Nature*. 397:50–53.

21. Tan, J. L., J. Tien, D. M. Pirone, D. S. Gray, K. Bhadriraju, and C. S. Chen. 2003. Cells lying on a bed of microneedles: an approach to isolate mechanical force. *Proc. Natl. Acad. Sci. USA*. 100:1484–1489.

22. Landau, L. D., and E. M. Lifshitz. 1988. Theory of Elasticity. Pergamon Press, Oxford, UK.

23. Sheu, M. T., J. C. Huang, G. C. Yeh, and H. O. Ho. 2001. Characterization of collagen gel solutions and collagen matrices for cell culture. *Biomaterials*. 22:1713–1719.

24. Evans, E. 2001. Probing the relation between force lifetime and chemistry in single molecular bonds. *Annu. Rev. Biophys. Biomol. Struct*. 30:105–128.